Nano Energy 31 (2017) 258–263

Contents lists available at ScienceDirect

Nano Energy

journal homepage: www.elsevier.com/locate/nanoen

Post ionized defect engineering of the screen-printed $Bi_2Te_{2.7}Se_{0.3}$ thick film for high performance flexible thermoelectric generator

Sun Jin Kim[a], Hyeongdo Choi[a], Yongjun Kim[a], Ju Hyung We[a], Ji Seon Shin[b], Han Eol Lee[c], Min-Wook Oh[d], Keon Jae Lee[c], Byung Jin Cho[a,*]

[a] Department of Electrical Engineering, KAIST, 291 Daehak-ro, Yuseong, Daejeon, Republic of Korea
[b] Tegway Co. Ltd., #711 National Nano Fab., 291 Daehak-ro, Yuseong-gu, 34141 Daejon, Republic of Korea
[c] Department of Materials Science and Engineering, KAIST, 291 Daehak-ro, Yuseong, Daejeon, Republic of Korea
[d] Department of Advanced Materials Engineering, Hanbat National University, Daejeon 34158, Republic of Korea

ARTICLE INFO

Keywords:
Screen-printed $Bi_2Te_{2.7}Se_{0.3}$ film
Post ionized defect engineering
Hydrogen annealing
Bismuth antisite defect

ABSTRACT

Flexible thermoelectric generators (f-TEGs), fabricated by the screen printing technique, have been introduced as a semi-permanent power source for wearable and flexible electronic systems. However, the output power density of the f-TEG module is still limited due to the low ZT of the screen-printed thermoelectric (TE) film. We herein report a post ionized defect engineering process that effectively controls ionized defects and improves the ZT value of a screen-printed ternary TE film. It was found that post annealing in a forming gas ambient (4% H_2+96% Ar) can reduce the nano- and micro-bismuth oxide particles in screen-printed n-type BiTeSe films, resulting in a bismuth rich condition and creation of bismuth antisite defects. We achieved a maximum ZT of 0.90 with the screen-printed n-type BiTeSe thick film at room temperature, which is almost comparable to that of the bulk $Bi_2Te_{2.7}Se_{0.3}$ and is a 2-fold increase over the same screen-printed film without the hydrogen ambient annealing. To demonstrate the applicability of this approach, a f-TEG device with 72 TE pairs (p-type $Bi_{0.5}Sb_{1.5}Te_3$, forming gas annealed n-type $Bi_2Te_{2.7}Se_{0.3}$) was fabricated by the screen printing technique. The device generated a high output power of 6.32 mW cm^{-2} at ΔT=25.6 °C. These results demonstrate the feasibility of high performance and large-scale f-TEG fabrication using ionized-defect engineering.

1. Introduction

Thermoelectric (TE) material engineering has been actively studied for high energy conversion efficiency and easy commercialization over the past several decades[1–5]. Among them, advanced printing technologies such as 3D printing [6–8] and screen printing processes [9–11] have attracted wide interest because they provide a number of advantages, including easy processing, large-scale manufacturing, high integration and mass production. Given such features, many researchers have attempted to fabricate flexible thermoelectric generators (f-TEG) using various printing processes. Printable f-TEG would be useful in a wide range of applications, particularly energy savings systems, power generators, and wearable and self-powered electronics. He et al. reported the fabrication of Bi_2Te_3-based amorphous TE materials with ultralow thermal conductivity using a 3D printing technique [12]. Jo et al. utilized a dispenser printing technology with a printable mixture consisting of a polymer binder and TE particles (n-type and p-type Bi_2Te_3) [13]. Lu et al. employed inkjet printing to fabricate flexible thermoelectric thin film devices containing p-type $Bi_{0.5}Sb_{1.5}Te_3$ and n-type $Bi_2Te_{2.7}Se_{0.3}$ nanoparticles [14]. However, these printed f-TEG modules have exhibited very lower output power densities, compared to bulk TEG. One significant barrier to achieving high output power density is the low ZT of the printed TE materials. Printed f-TEGs typically exhibit a low figure of merit because it is very difficult to control organic contamination and physical and chemical defects in the TE materials after the printing process. For that reason, controlling defects by using a post annealing process after printing is considered a key approach for enhancing the ZT of printed TE materials, and improving the output characteristics of f-TEGs.

In this paper, we report a novel method of enhancing the TE properties of a screen-printed $Bi_2Te_{2.7}Se_{0.3}$ thick film, post ionized defect (PID) engineering, which employs a forming gas (4% H_2+96% Ar) annealing (FGA) process. We achieved a maximum ZT of 0.90 in a screen-printed n-type $Bi_2Te_{2.7}Se_{0.3}$ thick film at room temperature. This performance is almost comparable to that of the bulk $Bi_2Te_{2.7}Se_{0.3}$ and is a 2-fold increase over the same screen-printed film without the hydrogen ambient annealing.

* Corresponding author.
E-mail address: bjcho@kaist.edu (B.J. Cho).

http://dx.doi.org/10.1016/j.nanoen.2016.11.034
Received 6 October 2016; Received in revised form 12 November 2016; Accepted 16 November 2016
Available online 18 November 2016

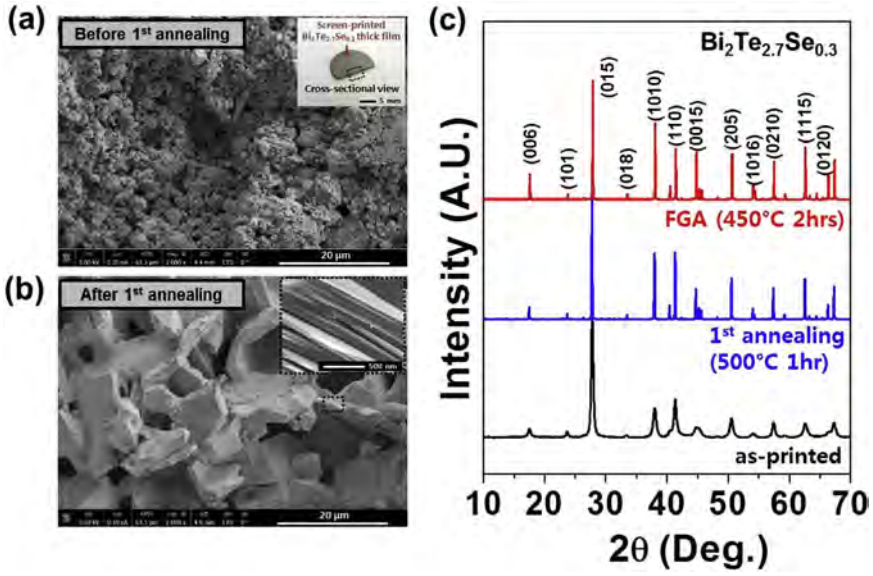

Fig. 1. (a) and (b) SEM images and (c) X-ray diffraction patterns of the screen-printed $Bi_2Te_{2.7}Se_{0.3}$ thick film before and after the 1st annealing step, and the FGA step (2nd annealing), respectively. The inset of Fig. 1a shows an actual photo of the screen-printed $Bi_2Te_{2.7}Se_{0.3}$ thick film. The inset of Fig. 1b is a high resolution SEM image.

2. Results and discussion

2.1. Microstructure and compositional analysis

The first step in the successful formation of the screen-printed $Bi_2Te_{2.7}Se_{0.3}$ thick film is the synthesis of a $Bi_2Te_{2.7}Se_{0.3}$ paste, consisting of a binder, glass frit, a solvent and TE materials (seeTable S1for details). The two organic materials, the binder and the solvent were mixed to improve the viscosity of the TE paste. The glass frit plays a critical role by providing nucleation centers for the recrystallization of the TE thick film.

Next, the TE paste was printed on an alumina substrate, and subjected to the 1st annealing step in a tellurium ambient. Here, extra tellurium powder (0.02 g) was placed adjacent to the screen-printed TE thick film to make a tellurium ambient. The annealing step in a tellurium ambient is illustrated inFig. S2.Fig. 1a and b show SEM images of the screen-printed $Bi_2Te_{2.7}Se_{0.3}$ thick film before and after the 1st annealing at 500 °C for 80 min in a tellurium ambient. The TE film before the 1st annealing is composed of a large number of ternary TE particles with various sizes and shapes. After the annealing process, however, the TE film shows randomly oriented thick TE flakes with a high degree of porosity, and a polycrystalline n-type $Bi_2Te_{2.7}Se_{0.3}$ phase (See Additional information in Fig. S1). The high resolution SEM images in the inset of Fig. 1b illustrate the lamellar structure of the $Bi_2Te_{2.7}Se_{0.3}$ thick film. Fig. 1c shows X-ray diffraction patterns of the TE thick films before and after the 1st annealing step, and the FGA process (2nd annealing) which was conducted at 450 °C for 2 h, respectively. The XRD data shows that the as-printed TE sample has broadened peaks in comparison with the annealed TE sample. This is because grain growth occurs during the 1st annealing. No significant change was observed after the FGA process, such as a phase change or material decomposition.

2.2. Thermoelectric properties via Hydrogen annealing

The thermoelectric properties of the screen-printed $Bi_2Te_{2.7}Se_{0.3}$ thick films treated at various FGA conditions are shown in Fig. 2. Details of the TE property measurements are described in the supplementary information. The TE properties were measured at room temperature. The Seebeck coefficient of the TE thick film increased by up to 50% (~190 μV K^{-1} from ~121 μV K^{-1}), while electrical conductivity decreased 48% (~47,700 S m^{-1} from ~89,960 S m^{-1}). Thermal conductivity fell to as low as 0.65 W $m^{-1}K^{-1}$ after the annealing process, with the same tendency as electrical conductivity, and the optimum ZT of 0.88 was observed at 450 °C. These results clearly show a trade-off relationship between the thermoelectric factors as a function of the post annealing conditions in a hydrogen ambient. The $Bi_2Te_{2.7}Se_{0.3}$ thick film electrically and thermally experiences a substantial change during the post annealing process above 450 °C. It is thought that the high temperature annealing above 450 °C accelerates the creation of ionized defects in the $Bi_2Te_{2.7}Se_{0.3}$ matrix, resulting in lower carrier concentration (seeFig. S3). The details of defect generation will be discussed in Fig. 3. The thermoelectric properties as a function of annealing time at 450 °C are shown in Fig. 2c and d. The results show the same trend as those obtained at different annealing temperatures. The Seebeck coefficient of the TE film increases linearly, while on the other hand, the electrical and thermal conductivities linearly decrease with annealing time. The maximum ZT of 0.90 at room temperature was obtained following FGA treatment at 450 °C for 4 h. The maximum ZT was 2-fold greater than that exhibited by a $Bi_2Te_{2.7}Se_{0.3}$ thick film which had not undergone the FGA process. The results shown in Fig. 2e and f indicate that all the thermoelectric factors are strongly coupled to carrier concentration, which agrees with the typical behavior of thermoelectrics [15].

2.3. Generation of antisite defects in $Bi_2Te_{2.7}Se_{0.3}$ matrix

In order to understand the mechanism behind the significant changes in carrier concentration that occurred during the hydrogen annealing, XRD analysis was carried out for TE samples prepared with different annealing conditions, and the results are shown in Fig. 3. The screen-printed $Bi_2Te_{2.7}Se_{0.3}$ thick film that was recrystallized by the 1st annealing step reveals a tellurium-rich film, but it subsequently changed to a tellurium-deficient film after the FGA treatment, because of the low vaporization energy of tellurium (Te). As shown in Fig. 3a and b, the XRD peaks corresponding to Te gradually decrease and then completely disappear as the FGA temperature or time increases. It may be that the FGA process increases the concentration of Te vacancy defects in the screen-printed $Bi_2Te_{2.7}Se_{0.3}$ thick film. However, vacancy defects, which provide two free electrons, cannot explain the reduction in electron concentrations observed in this study. Fig. 3 indicates the lattice parameters calculated from the XRD peak-shift. The lattice parameters of the a-axis show similar values, while those of the c-axis increase with annealing temperature and time, and this gives us an

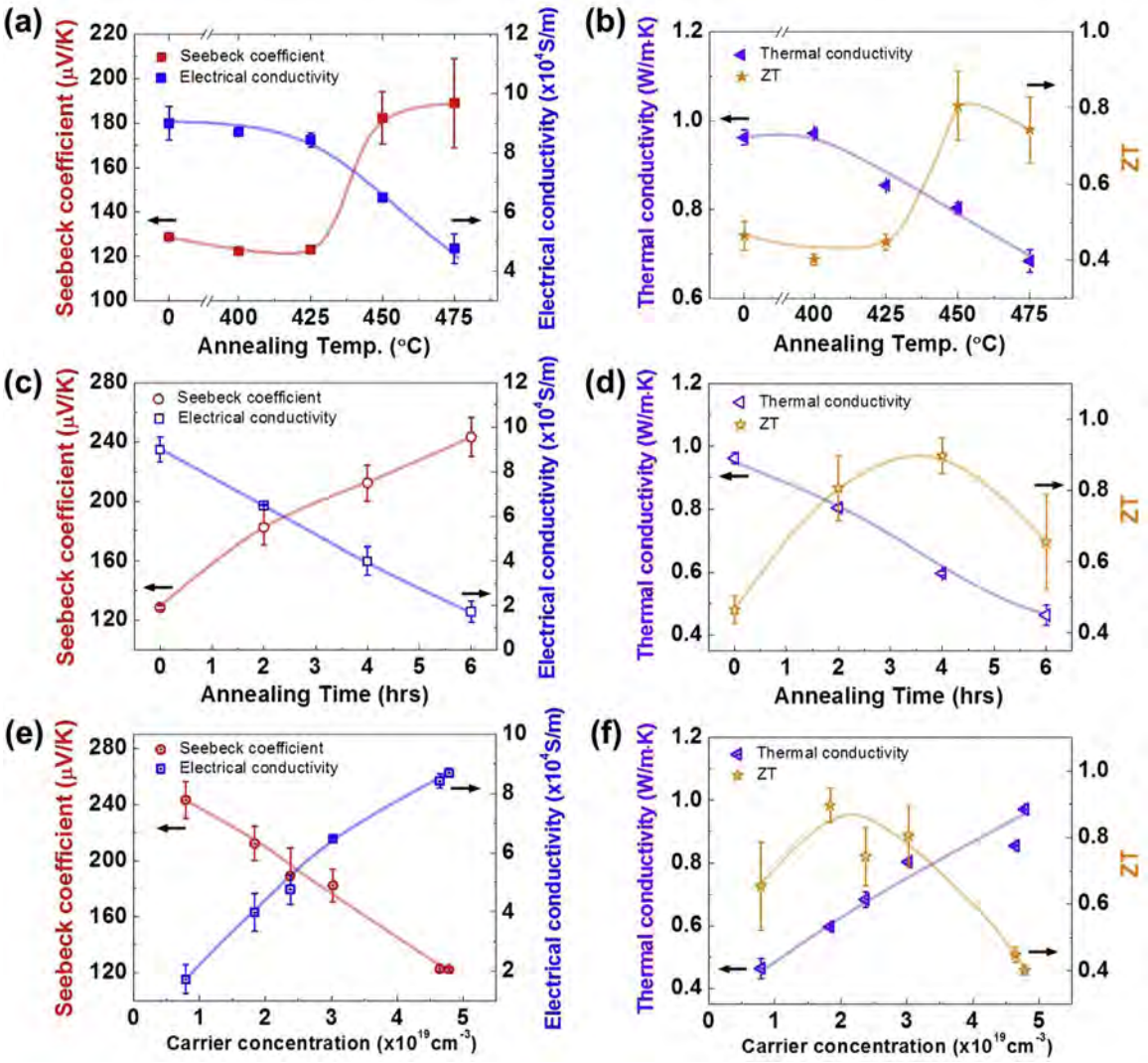

Fig. 2. Thermoelectric properties of the screen-printed $Bi_2Te_{2.7}Se_{0.3}$ thick film after the FGA process as a function of (a) and (b) annealing temperature, (b) and (d) annealing time and (e) and (f) carrier concentration at room temperature.

important clue. The increased lattice parameters of the c-axis can be attributed to the generation of bismuth antisite defects (Bi_{Te}) in the $Bi_2Te_{2.7}Se_{0.3}$ thick film: it is well known that the lattice parameters increase when the concentration of [Bi_{Te}] increases, since Bi has a larger atomic radius (1.6 Å) than Te (1.4 Å) [16–18]. Therefore, the increased content of Bi_{Te}, which is an electron acceptor, may cause the significant reduction in carrier concentration in the screen-printed $Bi_2Te_{2.7}Se_{0.3}$ thick film. The screen-printed $Bi_2Te_{2.7}Se_{0.3}$ thick film was investigated by back scattered electron (BSE) and energy-dispersive X-ray spectroscopy (EDX). Fig. 4b and c show the BSE images of the $Bi_2Te_{2.7}Se_{0.3}$ thick film, with surface and cross-sectional views. It can be seen that round-shaped particles ranging from nano- to micro-size (the dark-grey particles in Fig. 3b and c) are randomly scattered throughout the $Bi_2Te_{2.7}Se_{0.3}$ matrix. The results obtained by EDX demonstrate that the bright regions in the BSE images are $Bi_2Te_{2.7}Se_{0.3}$ material, but the dark-greyed particles are glass frit, composed of Bi_2O_3 with SiO_2, Al_2O_3 and ZnO (Fig. 3d). The glass frit was mixed with the TE powders in the early stage of the paste synthesis to promote recrystallization of the TE material during the thermal annealing. Fig. S4 proves that the composition of the glass frit is well matched with that of the dark-grey particles in the screen-printed $Bi_2Te_{2.7}Se_{0.3}$ matrix. It is also believed that the glass frit, which undergoes an oxide reduction process during the FGA treatment, partially contributes to the Bi-rich condition and leads to the creation of the antisite defects [Bi_{Te}], then reduces the electron concentration, as illustrated in Fig. 4a. Table S2 provides further information on the oxide reduction under hydrogen annealing. The atomic percent of oxygen declines to 17 at% after FGA treatment at 450 °C for 6 h, which is 2.5 times lower than the sample fabricated without the FGA process.

2.4. Output performance of a flexible TEG module

To verify that the actual power generation of the f-TEG can be improved by the ionized defect engineering process, we fabricated a 40 mm×40 mm×0.8 mm flexible TEG comprised of 72 TE pairs of $Bi_{0.5}Sb_{1.5}Te_3$ (*p*-type) legs and reduced Bi_2 $Te_{2.7}Se_{0.3}$ (*n*-type) legs, using the screen printing technique [19–21] and laser multi-scanning technique. For comparison, a control sample containing Bi_2 $Te_{2.7}Se_{0.3}$ (*n*-type) film was fabricated without the FGA process as well. The inset in Fig. 5a shows an actual photo of the flexible TEG. To measure the output characteristics, the flexible TEG was mounted between the hot and cold plates of a power measurement system. Once the temperature difference (△T) across the TEG device was in a thermally steady-state mode, the voltage-current characteristics were simultaneously measured as a function of the output voltage through a computer controlled multimeter and source meter. Then, the power curve was calculated from the product of the output current and the voltage of the device at a given △T (seeFig. S6). Fig. 5a presents the voltage-current curve

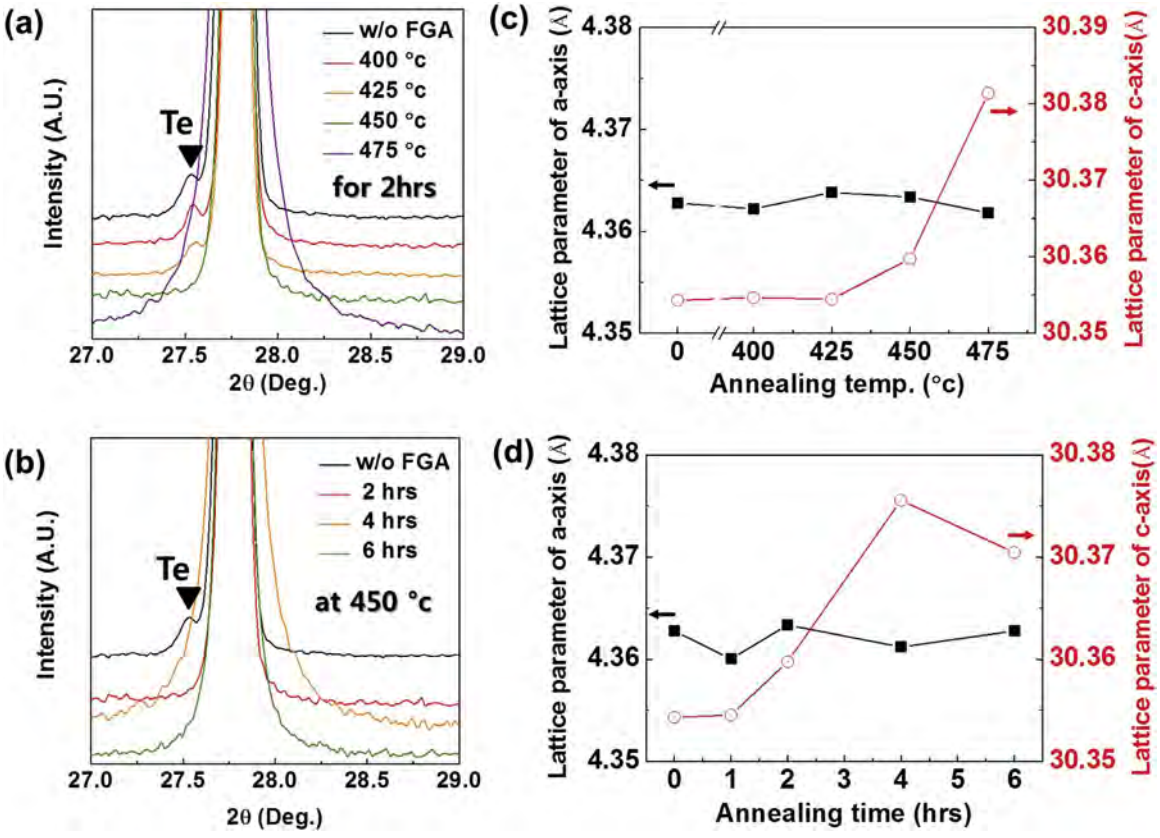

Fig. 3. (a) and (b) X-ray diffraction patterns and (c) and (d) lattice parameters of the screen-printed $Bi_2Te_{2.7}Se_{0.3}$ thick film as a function of annealing temperature and annealing time.

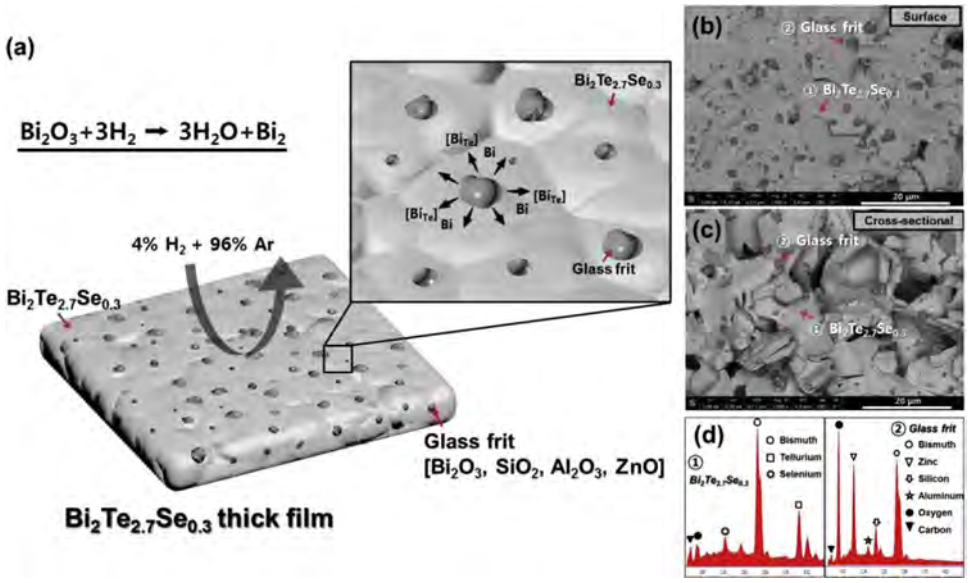

Fig. 4. (a) Schematic illustration of the ionized defect engineering of the $Bi_2Te_{2.7}Se_{0.3}$ film. SEM images of the screen-printed $Bi_2Te_{2.7}Se_{0.3}$ thick film (surface (b) and cross-sectional view (c)). (d) EDX spectra of the corresponding arrows in the BSE images.

(dashed lines) and the output power density (thick lines) with respect to △T. The open-circuit voltage is 693 mV, and the power density generated is about 6.32 mW cm^{-2} at a △T=25.6 °C, which is 40% and 30% higher than those of the control sample, respectively (Fig. 5b). This enhancement is due to the substantial increase in the Seebeck coefficient of the Bi_2 $Te_{2.7}Se_{0.3}$ (*n*-type) thick film after the FGA process, up to 220 μV K^{-1}. The measured power enhancement indicates that ionized defect engineering of the screen-printed TE film using the FGA process is a critical step in the development of a high-power f-TEG device.

3. Conclusion

In summary, our research group previously reported the fabrication of f-TEGs using screen-printed thick films, which showed a high output power density with excellent flexibility. However, the a-type $Bi_2Te_{2.7}Se_{0.3}$ thick film suffered from a low power factor of 1.69 Wm^{-1} K^{-2} and a ZT value of 0.57, resulting in a relatively low

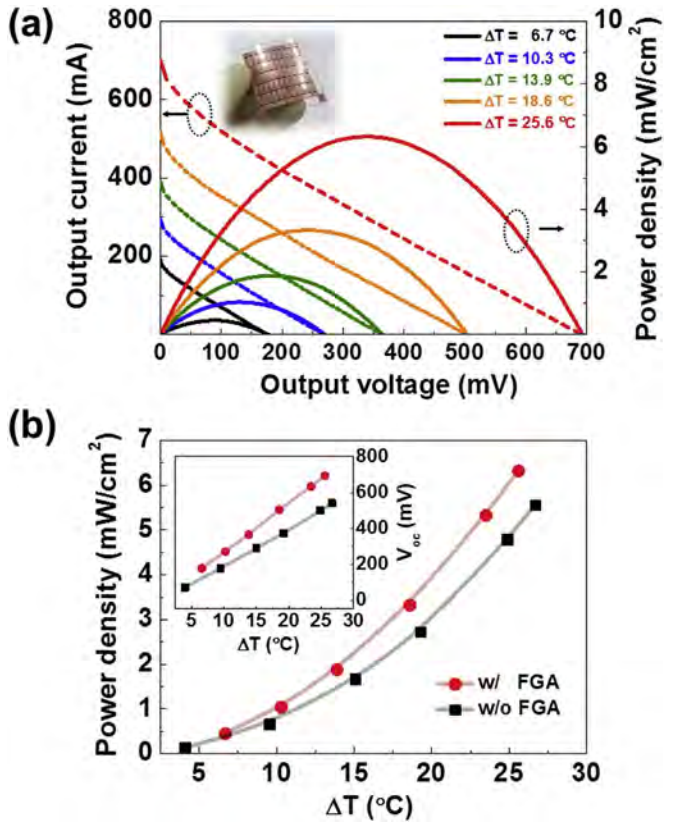

Fig. 5. Output characteristics of the flexible TEGs (72 TE pairs) with the reduced $Bi_2Te_{2.7}Se_{0.3}$ thick films versus the pristine $Bi_2Te_{2.7}Se_{0.3}$ thick films; (a) Current-voltage (I–V) curves (dashed lines) and output power density (thick lines) of the flexible TEG with the reduced $Bi_2Te_{2.7}Se_{0.3}$ thick films. (b) Comparison of power density of the two flexible TEGs as a function of ΔT. Inset shows the open circuit voltage of the two flexible TEGs.

output power density compared to a bulk Bi_2Te_3-based commercial TE generator. To enhance the performance of screen printed n-type film, a novel approach to effectively improve the ZT value of the screen-printed $Bi_2Te_{2.7}Se_{0.3}$ thick film using ionized defect engineering was introduced. The forming gas ambient annealing (FGA) processing of screen printed $Bi_2Te_{2.7}Se_{0.3}$ thick film enhanced the ZT value up to 0.90, which was 2-fold higher than that of the same film without the FGA process. A flexible TEG was also demonstrated using the ionized defect engineering process. Arrays of 72 pairs of $Bi_2Te_{2.7}Se_{0.3}$ legs were annealed in a hydrogen gas ambient. The fabricated f-TEG exhibited a power enhancement of 30% (6.32 mW cm^{-2} at ΔT=25.6 °C) compared to a control sample prepared without the FGA process. The process described in this work would be beneficial for the large-scale ionized-defect engineering of hundreds to thousands of $Bi_2Te_{2.7}Se_{0.3}$ arrays with good controllability, and provides an advantageous approach for manufacturing high performance f-TEGs.

Acknowledgement

This work was supported by the National Research Foundation of Korea (NRF) Grant funded by the Korean Government (MSIP). (NRF-2015R1A5A1036133).

Appendix A. Supplementary material

Supplementary data associated with this article can be found in the online version at http://dx.doi.org/10.1016/j.nanoen.2016.11.034.

References

[1] A.J. Minnich, M.S. Dresselhaus, Z.F. Ren, G. Chen, Energy Environ. Sci. 2 (2009) 466–479.
[2] B.C. Sales, D. Mandrus, R.K. Williams, Science, 272, 5266, 1325.
[3] X. Yan, B. Poudel, Y. Ma, W.S. Liu, G. Joshi, H. Wang, Y. Lan, D. Wang, G. Chen, Z.F. Ren, Nano Lett. 10 (2010) 3373–3378.
[4] A. Soni, Z. Yanyuan, Y. Ligen, M.K.K. Aik, M.S. Dresselhaus, Q. Xiong, Nano Lett. 12 (2012) 1203–1209.
[5] Y. Yang, Z.H. Lin, T. Hou, F. Zhang, Z.L. Wang, Nano Res. 5 (2012) 888–895.
[6] D. Kokkinis, M. Schaffner, A.R. Studart, Nat. Commun. 6 (2015) 8643.
[7] Q. Zhang, K. Zhang, G. Hu, Sci. Rep. 6 (2016) 22431.
[8] Z. Chen, X. Song, L. Lei, X. Chen, C. Fei, C.T. Chiu, X. Qian, T. Ma, Y. Yang, K. Shung, Y. Chen, Q. Zhou, Nano Energy 27 (2016) 78–86.
[9] M. Fekete, R.K. Hocking, S.L.Y. Chang, C. Italiano, A.F. Patti, F. Arena, L. Spiccia, Energy Environ. Sci. 6 (2013) 2222–2232.
[10] W.J. Hyun, E.B. Secor, M.C. Hersam, C.D. Frisbie, L.F. Francis, Adv. Mater. 27 (2015) 109–115.
[11] K. Cao, Z. Zuo, J. Cui, Y. Shen, T. Moehl, S.M. Zakeeruddin, M. Grätzel, M. Wang, Nano Energy 17 (2015) 171–179.
[12] M. He, Y. Zhao, B. Wang, Q. Xi, J. Zhou, Z. Liang, Small 11 (2015) 5889–5894.
[13] S.E. Jo, M.K. Kim, M.S. Kim, Y.J. Kim, Electron. Lett. 48 (2012) 1013–1015.
[14] Z. Lu, M. Layani, X. Zhao, L.P. Tan, T. Sun, S. Fan, Q. Yan, S. Magdassi, H.H. Hng, Small 10 (2014) 3551–3554.
[15] G.J. Snyder, E.S. Toberer, Nat. Mater. 7 (2008) 105–114.
[16] M.W. Oh, J.H. Son, B.S. Kim, S.D. Park, B.K. Min, H.W. Lee, J. Appl. Phys. 115 (2014) 133706.
[17] S. Cho, Y. Kim, A. DiVenere, G.K. Wong, J.B. Ketterson, Appl. Phys. Lett. 75 (1999) 1401.
[18] J.C. Slater, J. Chem. Phys. 41 (1964) 3199–3204.
[19] S.J. Kim, J.H. We, J.S. Kim, G.S. Kim, B.J. Cho, J. Alloy. Compd. 582 (2014) 177–180.
[20] S.J. Kim, J.H. We, B.J. Cho, Energy Environ. Sci. 7 (2014) 1959–1965.
[21] J.H. We, S.J. Kim, G.S. Kim, B.J. Cho, J. Alloy. Compd. 552 (2013) 107–110.

Sun Jin Kim is currently a Ph.D candidate in Nano Electronics and Energy Device Laboratory from KAIST, under the supervision of Prof. Byung Jin Cho. His research focuses on the synthesis of thermoelectric paste and the process development for wearable and flexible thermoelectric devices.

Hyeongdo Choi received his M.S. degree in Electrical Engineering from KAIST in 2016. Then he is currently pursuing Ph.D degree in Nano Electronics and Energy Device Laboratory at KAIST, under the supervision of Prof. Byung Jin Cho. His research interests include the synthesis of functional inorganic pastes with thermoelectric materials and the design and optimization of thermoelectric device.

Yongjun Kim is currently a MS candidate in Nano Electronics and Energy Device Laboratory at KAIST, under the supervision of Prof. Byung Jin Cho. His research focuses on the interface engineering to enhance electrical and thermal contact resistances of flexible thermoelectric device.

Ju Hyung We received his Ph.D degree in Electrical Engineering from KAIST in 2015. His research focuses on hybrid composite of organic and inorganic thermoelectric materials for flexible thermoelectric generator.

Jiseon Shin received her MS degree in Materials Science and Engineering (MSE) from KAIST in 2013. She joined TEGway Co., Ltd. as a researcher in 2014 where her current research focuses on manufacturing processes of flexible thermoelectric device.

Han Eol Lee is a Ph.D candidate in Materials Science and Engineering (MSE) from KAIST, under the supervision of Prof. Keon Jae Lee. His doctoral research topics focus on inorganic-based flexible optoelectonics and laser material interaction for flexible display.

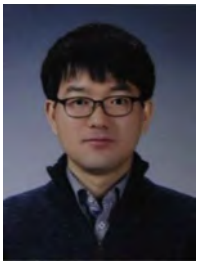

Min-Wook Oh is currently an assistant professor of Departmet of Advanced Materials Engineering at Hanbat National University, where he has been since 2015. He received his Ph.D in material science and engineering from KAIST in 2006. From 2005 to 2015 he worked as a senior reseacher at Korea Electrotechnology Research Insitute (KERI) and severed as a director of Thermoelectric Conversion Research Center at KERI from 2014 to 2015. His main research interests are the thermoelectirc materials, devices, and computational simulations.

Prof. Keon Jae Lee received his Ph.D in Materials Science and Engineering (MSE) at University of Illinois, Urbana-Champaign (UIUC). During his Ph.D at UIUC, he involved in the first co-invention of “Flexible Single-crystalline Inorganic Electronics”, using top-down semiconductors and soft lithographic transfer. Since 2009, he has been a professor in MSE at KAIST. His current research topics are self-powered flexible electronic systems including energy harvesting/storage devices, LEDs, large scale integration (LSI), high density memory and laser material interaction for in-vivo biomedical and flexible applications.

Prof. Byung Jin Cho received Ph.D degrees in electrical engineering from KAIST, Korea, in 1991. In 1991, he was with IMEC, Belgium, as a Research Fellow, where he worked on advanced silicon processing. In 1993, he joined SK Hynix Semiconductor. In 1997, he joined National University of Singapore, as a Faculty Member. Since 2007, he has been with KAIST. His main research interests are CMOS device and process technology, graphene-based devices, thermoelectric devices, and flexible electronics.